NUMERICAL INVESTIGATION OF SOLAR CELL TEMPERATURE FOR A CONCENTRATION OF PHOTOVOLTAIC SYSTEM

Kingley Aniekan Akai[1], *Rafiu Olalekan Kuku*[1], *Gbeminiyi Musibau Sobamowo* [2,*], *Nurudeen Adekunle Raji* [1]

[1]Department of Mechanical Engineering, Lagos State University, Epe, Lagos, Nigeria.
[2]Department of Mechanical Engineering, University of Lagos, Akoka, Lagos, Nigeria.

*Corresponding Author: Gbeminiyi Musibau Sobamowo (Email: mikegbeminiyiprof@yahoo.com)
(Received: 08-October-2024; accepted: 17-September-2025; published: 30-September-2025)
http://dx.doi.org/10.55579/jaec.202593.468

Abstract. *High operating temperatures of photovoltaic modules cause thermally-induced failures, degradation of the conversion efficiency and long-term reliability. As such, photovoltaic cells present limitations at high operating temperatures and anisotropic temperature distributions. Therefore, in order to maintain the temperature below the recommended operating temperature, there is a need for an effective cooling of the such power equipment. In this work, the thermal distribution in solar cells for a high concentration of photovoltaic system is numerically investigated using finite difference method. The parametric study in this work reveals significance of environmental parameters such as incident light, ambient conditions, wind velocity, and also material characteristics as well as the system size such as backplate emissivity, backplate coating, cell size, backplate thickness, and backplate length on the solar cell temperature. The solar cell temperature significantly reduces as the backplate thickness and emissivity, wind speed. However, reduction in backplate length potentially lower the cost and temperature of the solar cell. Also, increase in the incident light and ambient temperature cause increase in the solar cell temperature. It is anticipated that this work will contribute to an improved passive device design, particularly at the initial design stage when choosing the appropriate solar cell size and backplate thickness depending on the location of the project.*

Keywords: *Solar cells; backplate; photovoltaic; temperature distribution; finite difference method.*

1. Introduction

The potentials of photovoltaics (PV) in providing solutions to the current energy and environmental issues cannot be overemphasized. Solar cells which are photo-electric conversion semiconductors, are used in PV modules to directly convert absorbed solar radiation into electrical power. The continuous and expanding applications require further improvements in PV conversion efficiency and cost reduction in order to encourage the wide implementation of PV. Therefore, enhancing efficiency and improving lifetime are also important concerns in energy generation. One area of such improvement is in the cooling of the power component.

While most incident sunlight on the PV is absorbed by the solar cells, a significant amount of absorbed sunlight that is not able to be converted into electricity causes heat generation in the system, which consequently heats up the solar cells, electrodes, solders, wires, and sealants in the module, lowering system performance as a whole [1–3]. It was established that, the solar cell temperature (or module temperature) increases up to $50°C$ and higher for non-concentrated PVs [4–6] and $100°C$ for CPVs [7]. The PV module conversion efficiency and dependability are negatively impacted by this temperature rise. In fact, the present Si cells have a conversion efficiency of nearly 20% at room temperature ($25°C$), but for every degree Celsius that temperature rises, the relative efficiency decreases by about 0.45%, which is called temperature coefficient [3]. Therefore, as the temperature rises from $25°C$ to $60°C$, the efficiency drops from 20% to 17%. Moreover, it has been found that for every $10°C$ increase in operation temperature, the degradation rate of the PV module doubles [8]. Such high temperatures cause thermally-induced failures, degradation of the conversion efficiency and reduction long-term reliability of the PV module. As such, photovoltaic cells present limitations at high operating temperatures and anisotropic temperature distributions. Consequently, in order to maintain the temperature below the recommended operating temperature, improving long-term power generation performance and system reliability, there is a need for an effective PV module cooling method. As a response to this, various works has been presented in the literature on the cooling of PV modules [9–34]. Specifically, Wu et al. [34] presented an extensive indoor experimental investigation to characterize the heat loss from a point focus Fresnel lens PV Concentrator with a concentration ratio of 100×. The experiment was conducted for various ambient air temperatures, natural and forced convection, and a range of simulated solar radiation intensities between 200 and 1000 W/m^2. Some years later, Al-Amri et al. [10], developed a simple thermal model and presented a closed-form solution for the prediction of the solar cell temperature in the high concentration of photovoltaic system.

Indisputably, temperature and sun irradiation in particular have a significant impact on the performance of PV systems that are installed outdoors. As a result, it is essential to create precise prediction techniques for solar cells and modules that can examine how temperature changes and sun irradiation affect the electrical properties. These prediction techniques are essential for determining the potential energy output and for maximizing PV system performance in various environmental settings. To the best knowledge of the authors, a nonlinear thermal model which is a function of meteorological data and the optical, thermal, and electrical properties of the CPV system is not available in the literature. Therefore, in this work, nonlinear thermal models for predicting the concentration photovoltaic solar cell temperature distribution which is related meteorological data and the optical, thermal, and electrical properties of the CPV system were developed and analysed for a simple passive cooling method using a metal heat-spreading plate. Moreover, numerical solution of finite difference method represents an efficient way of calculating the temperature distribution in heat transfer processes. By segmenting the body into smaller domains, the FDM can be utilized to solve any complex body. Furthermore, a greater degree of approximation error removal can be achieved by selecting finer grids, which need significant processing power. Therefore, the finite difference method is used in this work. To analyze the developed thermal models. The significance of the model parameters such as incident light, ambient conditions, wind velocity, the system size, backplate emissivity, backplate coating, cell size, backplate thickness, and backplate length on the solar cell temperature are investigated and discussed.

2. Problem Formulation

Figure 1 presents high concentration of photovoltaic system. It is taken as depicted in the Figure 1a that every module in the system has the same heat transfer solutions because of their similar size and form. The virtual perpendicular dash lines in Figure 1b serve as adiabatic lines that separate the modules from one an-

other. Inside a single module, there is similarity in heat transfer between the four triangular areas confined between the two diagonal lines of the square plate, shown in Figure 1b. The two diagonal lines can be considered as adiabatic lines [10]. Thus, as illustrated in Figure 1c, the problem can be defined as heat transport through an extended fin with a trapezium form. As a result, the heat transfer model for the back plate will be developed based on the following assumptions.

1. The convection and radiation heat transfers from the solar cell to the environment are negligible compared to the conduction heat transfer to the backplate. This is because, at high values of the concentration ratio (the surface area ratio at the aperture and the receiver), the surface areas of solar cells are very small compared to the surface area of the aluminium backplate.
2. All the heat absorbed by the solar cell is transferred to the aluminium backplate through conduction.
3. The solar cell material is homogeneous and isotropic for the unidirectional heat conduction flow along the fin length.
4. The thermal and physical properties of the material for the solar cell are constant.
5. Thermal resistance and losses of conductive heat transfers in solar cell material and the adhesive layer are negligible. Thus, the heat transfer problem of the CPV system can be considered as a problem of heat transfer through a rectangular plate.
6. There is a uniform incident radiation on the surface area of the cells of the module.
7. A steady state heat transfer in the solar cell.

Using the stated assumptions, the thermal energy model are derived as follows

$$\begin{aligned}\text{Energy at the base} = {} & \text{energy out right face} \\ & + \text{energy lost by convection} \\ & + \text{energy lost by radiation}\end{aligned} \tag{1}$$

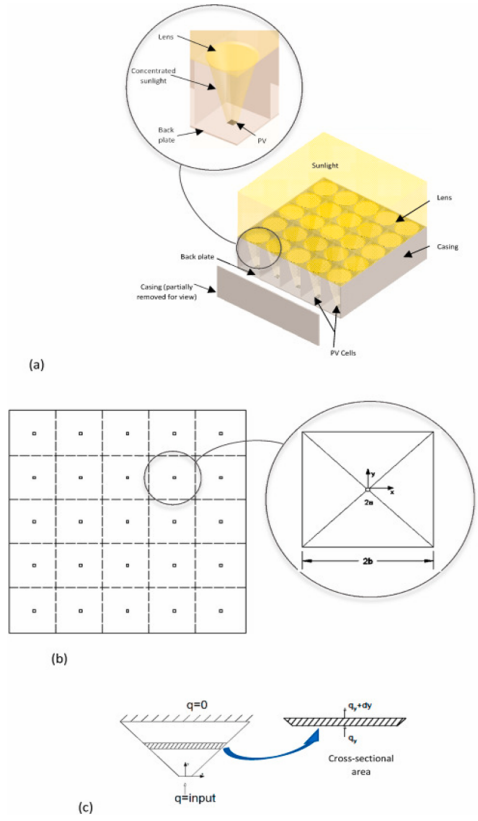

Fig. 1: The problem geometry: (a) high concentration of photovoltaic system considered (b) the top view of the solar cell and backplate top (c) the direction of heat transfer and the boundary conditions [10].

The mathematical representation of the Eq. (1) is

$$\begin{aligned}q_y = {} & \left(q_y + \frac{\partial q}{\partial y}\delta y\right) + h\frac{dA_{suf}}{dy}(T - T_a)\delta y \\ & + \sigma\varepsilon\frac{dA_{suf}}{dy}(T^4 - T_s^4)\delta y\end{aligned} \tag{2}$$

After collecting like terms, we have

$$-\frac{\partial q}{\partial y} = h\frac{dA_{suf}}{dy}(T - T_a) + \sigma\varepsilon\frac{dA_{suf}}{dy}(T^4 - T_s^4) \tag{3}$$

The heat conduction rate is given by Fourier's law as given

$$q = -kA_{cr}\frac{\partial T}{\partial y} \tag{4}$$

The introduction of Eq. (4) into Eq. (3) provides,

$$-\frac{\partial\left(-kA_{cr}\frac{\partial T}{\partial y}\right)}{\partial y}=h\frac{dA_{suff}}{dy}(T-T_a)+\sigma\varepsilon\frac{dA_{suff}}{dy}(T^4-T_s^4) \tag{5}$$

where

$$\begin{aligned} A_{cr}&=2t_c\,(y+a) \quad \Rightarrow \frac{dA_{cr}}{dy}=2t_c \\ A_{surf}&=2y\,(y+2a) \quad \Rightarrow \frac{dA_{surf}}{dy}=4(y+a) \end{aligned} \tag{6}$$

Therefore, Eq. (5) gives

$$\begin{aligned} 2kt_c\frac{\partial\left((y+a)\frac{\partial T}{\partial y}\right)}{\partial y}&=4h(y+a)(T-T_a) \\ &+4\sigma\varepsilon(y+a)(T^4-T_s^4) \end{aligned}$$

After expansion, we arrive at

$$\begin{aligned} &kt_c\,(y+a)\,\frac{\partial^2 T}{\partial y^2}+kt_c\frac{\partial T}{\partial y}= \\ &2h(y+a)(T-T_a)+2\sigma\varepsilon(y+a)(T^4-T_s^4) \end{aligned} \tag{7}$$

The above equation can be expressed as

$$\frac{\partial^2 T}{\partial y^2}+\frac{1}{(y+a)}\frac{\partial T}{\partial y}=\frac{2h(T-T_a)}{t_c k}+\frac{2\sigma\varepsilon(T^4-T_s^4)}{t_c k} \tag{8}$$

For the case when the temperature between the base and tip of the fin is small, the radiative term can be linearized. Using Roseland's approximation for the radiative term in the model, with the aid of Taylor series, expanding T^4 about T_a

$$T^4\cong T_a^4+4T_a^3\,(T-T_a)+6T_a^2(T-T_a)^2+4T_a(T-T_a)^3+\ldots \tag{9}$$

and ignoring the higher order components in Eq. (9), we have

$$T^4\cong 4T_a^3T-3T_a^4 \tag{10}$$

Therefore,

$$T^4-T_a^4\cong 4T_a^3(T-T_a) \tag{11}$$

Substituting Eq. (11) into Eq. (12) , we have

$$\frac{\partial^2 T}{\partial y^2}+\frac{1}{(y+a)}\frac{\partial T}{\partial y}=\frac{2h(T-T_a)}{t_c k}+\frac{8\sigma\varepsilon T_a^3(T-T_a)}{t_c k} \tag{12}$$

For the steady state heat transfer, we have

$$\frac{\partial^2 T}{\partial y^2}+\frac{1}{(y+a)}\frac{\partial T}{\partial y}-\frac{2h_{cr}(T-T_a)}{t_c k}=0 \tag{13}$$

where

$$h_{cr}=h+4\sigma\varepsilon T_a^3 \tag{14}$$

The respective heat transfer coefficient for the convection and radiation are given as [10]

$$\begin{aligned} h_c&=0.848k_a\sqrt{\frac{1}{d}\left(\frac{vPr\cos(w)}{\nu}\right)} \\ &=0.848\left(\sqrt{\frac{1}{bN}\left(\frac{vPr\cos(w)}{\nu}\right)}\right)k_a \end{aligned} \tag{15}$$

$$h_r=4\sigma\varepsilon T_a^3 \tag{16}$$

The combined heat transfer coefficient is the sum of the convection and radiation heat transfer coefficients, which is

$$h_{cr}=0.848\left(\sqrt{\frac{1}{bN}\left(\frac{vPr\cos(w)}{\nu}\right)}\right)k_a+4\sigma\varepsilon T_a^3 \tag{17}$$

Therefore, the thermal model becomes

$$\begin{aligned} &\frac{\partial^2 T}{\partial y^2}+\frac{1}{(y+a)}\frac{\partial T}{\partial y}- \\ &\frac{2\left(0.848\left(\sqrt{\frac{1}{b\cdot n}\left(\frac{vPr\cos(w)}{\nu}\right)}\right)k_a+4\sigma\varepsilon T_a^3\right)(T-T_a)}{t_c k}=0 \end{aligned} \tag{18}$$

The boundary conditions are

$$\frac{dT}{dy}=\frac{-a^2\times C\times I\times\eta_{opt}\,(1-\eta_{STC})}{2a\times k\times t_c}, \quad \text{at } y=0, \text{ for } t>0 \tag{19}$$

$$\frac{dT}{dy}=0, \text{ at } y=b-a, \text{ for } t>0 \tag{20}$$

As illustrated in Fig. 1b, only a quarter of the heat flux via the x-direction is examined due to the symmetry of the geometry under consideration. The boundary conditions represented in equations (19) and (20) depict the conditions seen in Figure 1c. It displays the heat flux value that is transported from the solar cell to the plate as well as the adiabatic value at the trapezoid's longer and shorter bases, respectively. (9a)

3. Method of Solution

While Eq. (18) is a nonlinear differential equation, Eq. (18) is a linear differential equation

with variable coefficient. It is very difficult to establish the exact solution of the nonlinear model. The use and the accuracy of finite difference method for the analysis of nonlinear problems has earlier been pointed out by Han et al. (2005). Therefore, in this work, finite difference method is used to discretize the governing Eq. (8) combined with the boundary conditions of Eq. (19) and (18). The finite difference forms or schemes for the differentials in the governing differential equations are given as

$$\frac{d^2T}{dy^2} = \frac{T_{i+1} - 2T_i + T_{i-1}}{(\Delta y)^2} \tag{21}$$

$$\frac{dT}{dy} = \frac{T_{i+1} - T_i}{\Delta y} = \frac{T_{i+1} - T_{i-1}}{2\Delta y} = \frac{T_i - T_{i-1}}{\Delta y} \tag{22}$$

Substituting the above finite difference schemes into Eq. (21) and (22) into the developed models in Eqs. (8) and (18), we obtain equivalent finite difference scheme as

For the nonlinear model

$$\frac{T_{i+1} - 2T_i + T_{i-1}}{(\Delta y)^2} - \frac{2\left(0.848\left(\sqrt{\frac{1}{bN}\left(\frac{vPr\cos(w)}{\nu}\right)}\right)k_a\right)(T_i - T_a)}{t_c k} + \frac{1}{(i\Delta y + a)}\left(\frac{T_{i+1} - T_i}{\Delta y}\right) - \frac{2\sigma\varepsilon(T_i^4 - T_s^4)}{t_c k} = 0 \tag{23}$$

After collecting the like terms, we have

$$\left(\frac{1}{(\Delta y)^2} + \frac{1}{(i\Delta y + a)\,\Delta y}\right)T_{i+1} - \frac{2\sigma\varepsilon}{t_c k}T_i^4 + \frac{1}{(\Delta y)^2}T_{i-1} + \left(\frac{2T_i}{(\Delta y)^2} + \frac{1}{(i\Delta y + a)\,\Delta y} + \frac{2\left(0.848\left(\sqrt{\frac{1}{bN}\left(\frac{vPr\cos(w)}{\nu}\right)}\right)k_a\right)}{t_c k}\right)T_i = -\left[\frac{2\left(0.848\left(\sqrt{\frac{1}{bN}\left(\frac{vPr\cos(w)}{\nu}\right)}\right)k_a\right)}{t_c k}T_a + \frac{2\sigma\varepsilon}{t_c k}T_s^4\right] \tag{24}$$

linear thermal model with variable coefficient

$$\frac{T_{i+1} - 2T_i + T_{i-1}}{(\Delta y)^2} + \frac{1}{(i\Delta y + a)}\left(\frac{T_{i+1} - T_i}{\Delta y}\right) - \frac{2\left(0.848\left(\sqrt{\frac{1}{bN}\left(\frac{vPr\cos(w)}{\nu}\right)}\right)k_a + 4\sigma\varepsilon T_a^3\right)(T_i - T_a)}{t_c k} = 0 \tag{25}$$

After collecting the like terms, we get

$$\left(\frac{1}{(\Delta y)^2} + \frac{1}{(i\Delta y + a)\,\Delta y}\right)T_{i+1} + \frac{1}{(\Delta y)^2}T_{i-1} + \left(\frac{2}{(\Delta y)^2} + \frac{1}{(i\Delta y + a)\,\Delta y} + \frac{\left\{2\left(0.848\left(\sqrt{\frac{1}{bN}\left(\frac{vPr\cos(w)}{\nu}\right)}\right)k_a\right) + 4\sigma\varepsilon T_a^3\right\}}{t_c k}\right)T_i = -\left[\left(\frac{\left\{2\left(0.848\left(\sqrt{\frac{1}{bN}\left(\frac{vPr\cos(w)}{\nu}\right)}\right)k_a\right) + 4\sigma\varepsilon T_a^2\right\}}{t_c k}\right)T_a\right] \tag{26}$$

The finite difference discretization for of the boundary conditions are

$$T_2 = T_0 + 2\left(\frac{-a^2 \times C \times I \times \eta_{opt}\,(1 - \eta_{STC})}{2a \times k \times t_c}\right)\Delta y \tag{27}$$

$$T_{M-1} = T_{M+1},\ \text{at}\ i = M \tag{28}$$

The algebraic evaluations of the numerical scheme of Eq. (26) with the boundary conditions in Eqs. (27) and (28) are solved using MATLAB. The results from the nodal points considered are plotted for verification and validations as shown in the next section.

4. Results and Discussion

The solutions of the developed numerical method were validated and then also verified with the experimental investigation by Wu et al. [34] and analytical solutions by Al-Amri et al. [10]. Figures. 1-5 depict the variation of the solar cell temperature with the solar irradiance from the present numerical solution and the published experimental work of [34]. As it could been seen that the results of the present study agree very well with the results of the experiment as presented in the literature.

Also, Figures 6-9 present the variation of the solar cell temperature with the solar irradiance from the present numerical solution of the linear thermal model and the published analytical solution of Al-Amri [10]. The analytical solution in the literature also verified the numerical solution in the present study. It should be noted that all the parameters used for the simulations in the present study are form the work of Wu et al. [34] and Al-Amri et al. [10].

The significance of emissivity on the solar cell temperature for four different values of ambi-

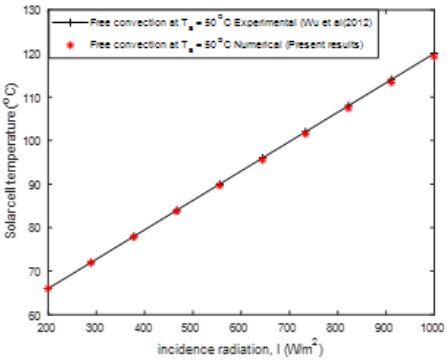

Fig. 2: Comparison of the experimental and the present numerical results of free convection at an ambient temperature of 50^oC.

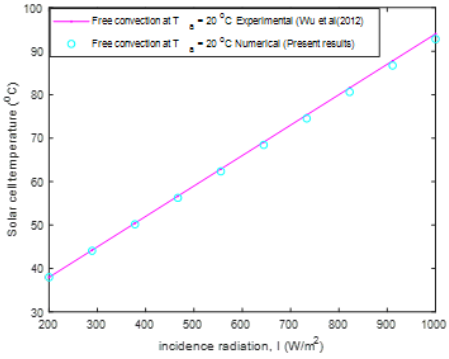

Fig. 3: Comparison of the experimental and the present numerical results of free convection at an ambient temperature of 20^oC.

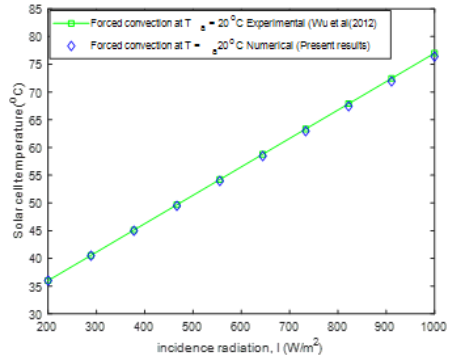

Fig. 4: Comparison of the experimental and the present numerical results of forced convection at an ambient temperature of 50^oC.

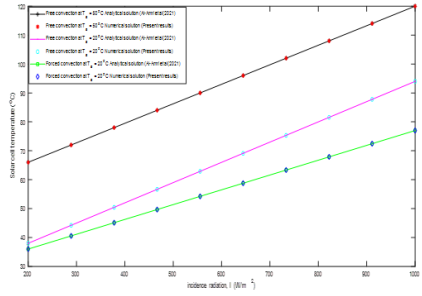

Fig. 5: Comparison of the experimental and the present numerical results of the linear models for free and forced convection at an ambient temperature of 20^oC and 50^oC.

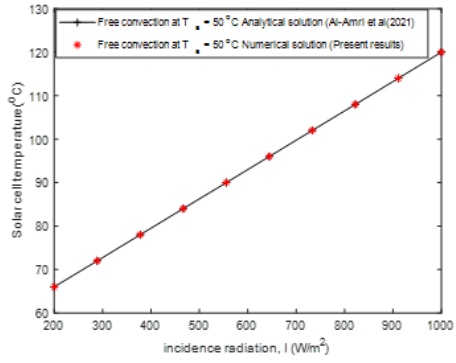

Fig. 6: Comparison of analytical and the present numerical results for the linear model of free convection at an ambient temperature of 50^oC.

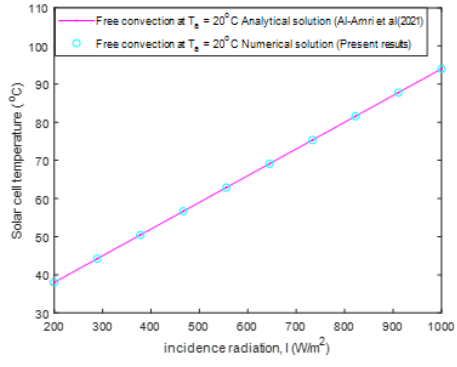

Fig. 7: Comparison of analytical and the present numerical results for the linear model of free convection at an ambient temperature of $50°C$.

ent temperature is illustrated in Figure 10. The results demonstrated that heat transfer by radiation reduces the temperature of a solar cell. Furthermore, it was established that the cell temperature consistently exceeded the accept-

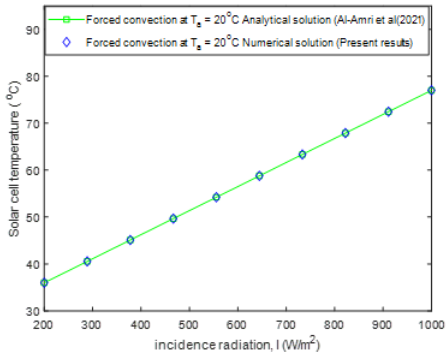

Fig. 8: Comparison of analytical and the present numerical results for the linear model of forced convection at an ambient temperature of 20^oC.

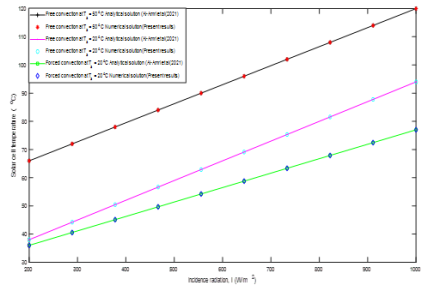

Fig. 9: Comparison of analytical and the present numerical results of the linear models for free and forced convection at an ambient temperature 20^oC and 50^oC.

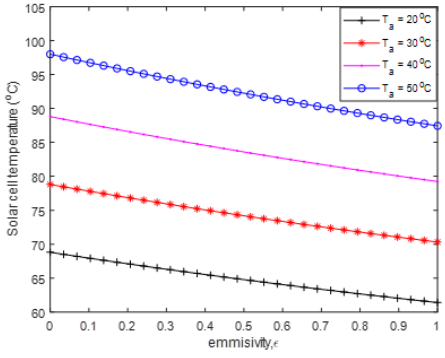

Fig. 10: Effects of emissivity on the solar cell temperature at different ambient temperature.

able threshold of $80°C$ in a harsh/hostile environment ($50°C$). This result indicates that the solar cell will deteriorate more quickly. On the other hand, at $40°C$, the gray backplate surface's surface radiation can assist in running the concentrated photovoltaic system below the advised safe temperature. Despite the backplate's emissivity, the working temperature is always below $80°C$ in mild weather of ambient temperature of $20°C$ and $30°C$ as illustrated in the figure.

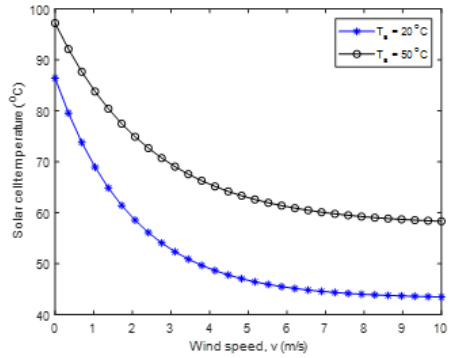

Fig. 11: Effects of wind speed on the solar cell temperature at different ambient temperature.

Figure 11 shows the impact of the wind speed under two different ambient temperatures on the temperature of the solar cell. It is shown that the solar cell temperature decreases significantly as the wind speed increases. This is because high wind speeds increase high convection heat transfer coefficient. Therefore, as the wind speed increase, the coefficient of heat transfer increases which consequently causes increased cooling of the solar cell and thereby decreases its temperature. It should be noted that the rate of reduction rate of temperature decreases with higher wind velocities and reaches a steady rate at a high value of the wind speed.

Figure 12 presents the effect of backplate length on the temperature of the solar cell under different ambient temperature. It is shown in the figure that the solar cell temperature significantly decreases with the backplate length. Although, using backplate of longer length seems desirable to make the solar cell operate below the established threshold temperature of $80°C$, it should be well noted that increasing the size of the backplate means higher initial cost and increased power consumption which will be required for tracking. Therefore, there is a need to determine an optimal length that results in the

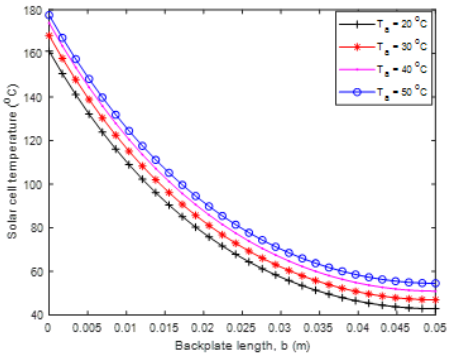

Fig. 12: Effects of backplate length on the solar cell temperature at different ambient temperature.

maximum net power output and minimum cost of the system.

Also, it could be established that the initial cost of the system can be decreased by reducing the backplate length, which also increases solar cell airflow and lowers cell temperature. Smaller cell sizes are more suited for harsh environment with ambient temperatures above $40°C$. This facilitates the control of the cell temperature drop below the $80°C$ threshold value.

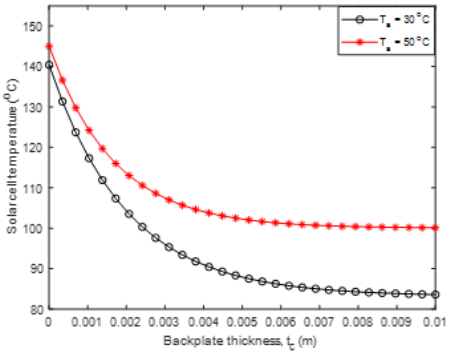

Fig. 13: Effects of backplate thickness on the solar cell temperature at different ambient temperature.

As the backplate thickness increases, the temperature of the solar cell decreases rapidly until the thickness after 8mm of the backplate thickness that the solar cell temperature becomes constant as depicted in Figure 13. However, it is shown that regardless of plate thickness, in a severe/harsh environment, the cell temperature always rises above the safe operating value. Although the thicker the plate thickness, the lower the solar cell temperature and that means higher initial cost and increased power consumption which will be required for tracking. Therefore, there is a need to determine an optimal length that results in the maximum net power output and minimum cost of the system.

5. Conclusion

The thermal distribution in solar cells for a high concentration of photovoltaic system has been modelled and solved numerically using finite difference method. The results of the numerical solutions were validated and then also verified with the experimental investigation and analytical solutions, respectively. The results demonstrated that the wind speed and heat transfer by radiation reduces the temperature of a solar cell. The solar cell temperature significantly decreases with the backplate length. As the backplate thickness increases, the temperature of the solar cell decreases rapidly until the thickness after 8 mm of the backplate thickness that the solar cell temperature becomes constant. Although, using backplate of longer length and larger thickness are seen as desirable to make the solar cell operate below the established threshold temperature, such will result in higher initial cost and increased power consumption which will be required for tracking. Therefore, there is a need to determine an optimal length that results in the maximum net power output and minimum cost of the system. It is expected that this work would improve the design of passive devices, especially in the early stages of selecting the right backplate thickness and solar cell size based on the project's location.

Nomenclature

η_{opt}	optical efficiency of the Fresnel lens
η_{STC}	electrical efficiency at STC
ν	kinematic viscosity of air, $m^2.s^{-1}$
σ	Stefan–Boltzmann constant (5.67×10^{-8} W m^{-2} K^{-4})
ε	emissivity of aluminium backplate

A_{cr} cross-sectional area, which varies with y, m^2

A_{surf} surface area of the differential element, m^2

h_c a function of wind speed and direction

I incident radiation, $W.m^{-2}$

k backplate thermal conductivity, $W.m^{-1}.K^{-1}$

k_a thermal conductivity of air, $0.026 W m^{-1} K^{-1}$

N number of solar cells (or modules) in each row

Pr Prandtl number of air

T temperature at any point in the plate, K

T_a ambient temperature T_∞

T_c backplate thickness, m

v wind speed, $m.s^{-1}$

w wind direction, degrees

a half of the solar cell length, m

b half of aluminium backplate length for each module, m

C concentration ratio, found in: $C = b^2/a^2$

d half length of the surface, m

h combined heat transfer coefficient, $W/(m^2.K)$

References

[1] E. Radziemska and E. Klugmann. Thermally affected parameters of the current–voltage characteristics of silicon photocell. *Energy Convers. Manag.*, 43(14):1889–1900, 2002.

[2] E. Radziemska. The effect of temperature on the power drop in crystalline silicon solar cells. *Renew. Energy*, 28(1):1–12, 2003.

[3] E. Skoplaki and J. A. Palyvos. On the temperature dependence of photovoltaic module electrical performance: A review of efficiency/power correlation. *Sol. Energy*, 83(5):614–624, 2009.

[4] A. D. Jones and C. P. Underwood. A thermal model for photovoltaic systems. *Sol. Energy*, 70(4):349–359, 2001.

[5] A. Akbarzadeh and T. Wadowski. Heat pipe-based cooling systems for photovoltaic cells under concentrated solar radiation. *Appl. Therm. Eng.*, 116(1):81–87, 1996.

[6] A. Royne and C. Dey. Design of a jet impingement cooling device for densely packed pv cells under high concentration. *Sol. Energy*, 81(8):1014–1024, 2007.

[7] B. J. Brinkworth, B. M. Cross, R. H. Marshall, and H. X. Yang. Thermal regulation of photovoltaic cladding. *Sol. Energy*, 61(3):169–178, 1997.

[8] P. Valeh-E-Sheyda, M. Rahimi, A. Parsamoghadam, and M. M. Masahi. Using a wind-driven ventilator to enhance a photovoltaic cell power generation. *Energy Build.*, 73:115–119, 2014.

[9] I. Ceylan, A. E. Gürel, H. Demircan, and B. Aksu. Cooling of a photovoltaic module with temperature controlled solar collector. *Energy Build.*, 72:96–101, 2014.

[10] F. G. Al-Amri and T. I. M. Abdelmagid. Analytical model for the prediction of solar cell temperature for a high-concentration photovoltaic system. *Case Stud. Therm. Eng.*, 25:100890, 2021.

[11] M. A. Bashir, H. M. Ali, K. P. Amber, M. W. Bashir, A. Hassan, S. Imran, and M. Sajid. Performance investigation of photovoltaic modules by back surface water cooling. *Therm. Sci.*, pages 1–110, 2016.

[12] B. Koteswararao, K. Radha, P. Vijay, and N. Raja. Experimental analysis of solar panel efficiency with different modes of cooling. *Int. J. Eng. Res. Dev.*, 8(3):1451–1456, 2016.

[13] M. Hasanuzzaman. Global advancement of cooling technologies for pv systems: a review. *Sol. Energy*, 137:25–45, 2016.

[14] D. Du, J. Darkwa, and G. Kokogiannakis. Thermal management systems for photovoltaics (pv) installations: a critical review. *Sol. Energy*, 97:238–254, 2013.

[15] H. G. Teo, P. S. Lee, and M. N. Hawlader. An active cooling system for photovoltaic modules. *Appl. Energy*, 90:309–315, 2012.

[16] S. Wu and C. Xiong. Passive cooling technology for photovoltaic panels for domestic houses. *Int. J. Low Carbon Technol.*, 9:118–126, 2014.

[17] M. Salih. Performance enhancement of pv array based on water spraying technique. *Int. J. Sustain. Green Energy*, 2014.

[18] Z. A. Haidar, J. Orfi, and Z. Kaneesamkandi. Experimental investigation of evaporative cooling for enhancing photovoltaic panels efficiency. *Results Phys.*, 11:690–697, 2018.

[19] S. Y. A. Wu, Q. L. Zhang, L. X. Xiao, and F. H. Guo. A heat pipe photovoltaic/thermal (pv/t) hybrid system and its performance evaluation. *Energy Build.*, 43:3558–3567, 2011.

[20] S. Mehrotra, P. Rawat, M. Debbarma, and K. Sudhakar. Performance of a solar panel with water immersion cooling technique. *Int. J. Sci. Environ. Technol.*, 3:1161–1172, 2014.

[21] K. A. S. Moharram, H. Abd-Elhady, M. S. Kandil, and A. H. El-Sherif. Enhancing the performance of photovoltaic panels by water cooling. *Ain Shams Eng. J.*, 4:869–877, 2013.

[22] M. R. Salem, M. M. Elsayed, A. A. Abd-Elaziz, and K. M. Elshazly. Performance enhancement of the photovoltaic cells using al2o3/pcm mixture and/or water cooling-techniques. *Renew. Energy*, 138:876–890, 2019.

[23] X. Tang, Z. Quan, and Y. Zhao. Experimental investigation of solar panel cooling by a novel micro heat pipe array. *Energy Power Eng.*, 2:171–174, 2010.

[24] L. Jaafer Habeeb, D. Ghanim Mutasher, and F. Abid Muslim Abd Ali. Cooling photovoltaic thermal solar panel by using heat pipe at baghdad climate. *Int. J. Mech. Mechatronics Eng.*, 17(6):171–185, 2017.

[25] N. Parkunam, L. Pandiyan, G. Navaneethakrishnan, S. Arul, and V. Vijayan. Experimental analysis on passive cooling of flat photovoltaic panel with heat sink and wick structure. *Energy Sources, Part A: Recover. Util. Environ. Eff.*, 2019.

[26] M. Firoozzadeh, A. H. Shiravi, and M. Shafiee. An experimental study on cooling the photovoltaic modules by fins to improve power generation: economic assessment. *Iran. (Iran.) J. Energy Environ.*, 10(2):80–84, 2019.

[27] Z. Arifin, D. D. D. P. Tjahjana, S. Hadi, R. A. Rachmanto, S. Gabriel, and B. Sutanto. Numerical and experimental investigation of air cooling for photovoltaic panels using aluminum heat sinks. *Int. J. Photoenergy*, page 1574274, 2020.

[28] S. Saadi, S. Benissaad, S. Poncet, and Y. Kabar. Effective cooling of photovoltaic solar cells by inserting triangular ribs: a numerical study. *Int. J. Energy Environ. Eng.*, 12(7):488–494, 2018.

[29] M. Ali, H. Ali, W. Moazzam, and M. B. Saeed. Performance enhancement of pv cells through micro-channel cooling. *AIMS Energy*, 3(4):699–710, 2015.

[30] L. Zhu, A. Raman, K. X. Wang, M. A. Anoma, and S. Fan. Radiative cooling of solar cells. *Optica*, 1, 2014.

[31] O. M. Ali, T. S. Maka, and O'Donovan. A review of thermal load and performance characterisation of a high, concentrating photovoltaic (hcpv) solar receiver assembly. *Sol. Energy*, 206:35–51, 2020.

[32] F. J. G. Gallero, I. R. Maestre, H. Hemida, and P. Á. Gómez. Practical approaches to assess thermal performance of a finned heat sink prototype for low concentration photovoltaics (lcpv) systems: analytical correlations vs cfd modelling. *Appl. Therm. Eng.*, 156:220–229, 2019.

[33] A. R. Gentle and G. B. Smith. Is enhanced radiative cooling of solar cell modules worth pursuing? *Sol. Energy Mater. Sol. Cells*, 150:39–42, 2016.

[34] Y. Wu, P. Eames, T. Mallick, and M. Sabry. Experimental characterisation of a fresnel lens photovoltaic concentrating system. *Sol. Energy*, 86(1):430–440, 2012.

About Authors